Corrosion fatigue behavior of Ti-6Al-4V: chemical and mechanical driving forces

E.V. Arcieri[1,2], S. Baragetti[1,2 *]
[1]*GITT - Centre on Innovation Management and Technology Transfer, University of Bergamo, Via Salvecchio 19, Bergamo 24129, Italy*
[2]*Department of Management, Information and Production Engineering, University of Bergamo, Viale Marconi 5, Dalmine 24044, Italy*

* Corresponding author
E-mail address: sergio.baragetti@unibg.it (S. Baragetti)

Abstract
The high strength-to-mass ratio and the appreciable corrosion resistance make the Ti-6Al-4V alloy used in aerospace, automotive, maritime and biomedical applications. In this work the quasi-static behavior of this light alloy and its axial fatigue resistance in air, air + beeswax coating, paraffin oil, 3.5wt.% NaCl solution and various water-methanol solutions are presented in order to understand the effects of the medium and of the load. The contribution of the stress concentration factor K_t, calculated by means of finite element modelling, is investigated. A SEM (scanning electron microscopy) analysis was carried out in order to evaluate the microstructural modifications due to the environments and cyclic loads.

Keywords: Ti-6Al-4V, corrosion fatigue, stress corrosion cracking, aggressive environment

1. Introduction

Thanks to its high mechanical and corrosion resistance the bimodal Ti-6Al-4V alloy is a very interesting challenge for several applications in automotive, aerospace, naval and biomedical engineering fields. Unfortunately, as stated in Brown [1] and Lee *et al.* [2], these features can decrease in presence of damages of the passivating TiO2 surface layer caused by low adhesion on the sublayer, variable loads and aggressive environments. Some tests carried out by Johnston [3] and Johnson [4] on pressurized fuel tanks for the Apollo mission pointed out the aggressiveness of the methanol on this alloy. For this reason, the Scientific Community is very attracted by this alloy as demonstrated by the substantial quantity of literature data collected by Brown [1], Lee *et al.* [2], Morrissey [5], Ritchie *et al.* [6], Morrissey [7] and Lanning *et al*. [8-9].

Moreover, fatigue and the determination of the remaining lifetime of a mechanical component is an interesting issue as stated in Gubeljak *et al*. [10].

In Morrisey *et al.* [7] the Haigh diagram for smooth cylindrical specimens in ultrasonic fatigue tests were obtain while in Lanning *et al.* [9] smooth and notched samples with different stress concentration factors were tested for a life of 1,000,000 cycles. Bellows *et al.* [11] carried out several tests in order to validate the step loading procedure were carried out for smooth specimens, showing high dispersion of values for R=0.1. The resulting fatigue strength to 10,000,000 cycles was reported. Haritos *et al.* [12] calculated the fatigue limit of smooth cylindrical samples for 10,000,000 cycles. In Peters *et al.* [13] the foreign-object damage on a Ti-6Al-4V turbine subjected to high cycles fatigue was investigated.

Furthermore, additive manufacturing is a good challenge in aerospace applications because it allows to obtain light components, as stressed also in Leuders *et al.* [14] and Kahlin *et al.* [15] even if the fatigue strength is not comparable to the one obtainable with the common technological procedures. Leuders *et al.* [14] studied the effects of the porosity on the fatigue behavior of additive manufactured Ti-6Al-4V specimens which gives a detrimental reduction of the strength. Kahlin *et al.* [15] showed instead how the Cumulative damage approach could be applied to predict fatigue life for additive manufactured samples subjected to prevalent tensile load tests.

Seifi *et al.* [16] studied Ti-6Al-4V specimens factory-made by electron beam melting (EBM) and the effects of a following hot isostatic pressing (HIP) analyzing also the microstructure of the samples concluding that in general their fatigue behavior was similar to the cast and wrought Ti-6Al-4V.

The behavior of Ti-6Al-4V alloy in terms of crack propagation in such different environments is shown in Dawson and Pelloux [17]. Three different trends of crack propagation were discovered in relation to the frequency of the applied load and the medium in which the specimen was immersed (Figure 1). The first one is frequency independent and is typical of the alloy in vacuum, air and solutions with corrosion inhibitors. In presence of methanol the propagation rate decreases when frequency increases. The reason of this behavior can be identified in the minor time available for the corrosive attack between two peaks of load. The last behavior shows a trend inversion in correspondence of ΔK_{scc} and is the compromise of the repassivating action and the effects of the frequency. Ti-6Al-4V presents this behavior in saline and potassium bromide solutions.

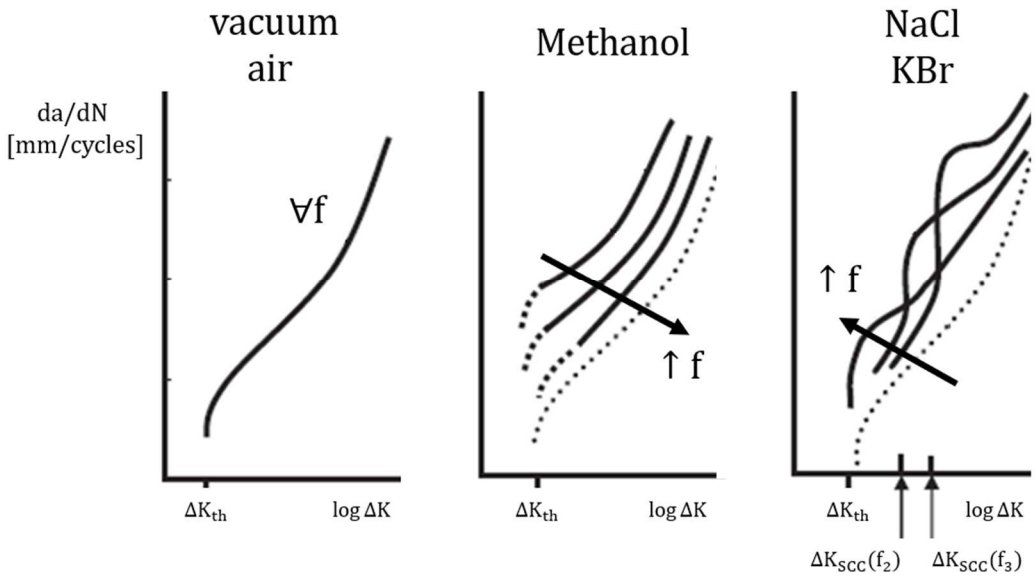

Figure 1 Crack propagation vs load frequency and environment, adapted from *[17]*.

Dawson and Pelloux [17] investigated also the effects of the load shape: sinusoidal loads have less detrimental effects than rectangular loads because in the first case the time available for the corrosion attacks is minor than the second case.

In Htoo [18] fatigue tests with load ratio equal to 0.1 were carried out on notched Ti-6Al-4V samples in order to evaluate the region between the low and high cycle fatigue pointing out a variation of the local stress ratio at notch root from -1 (low cycle) and 0.1 (high cycle).

The Structural Mechanics Laboratory – SMLab – of the University of Bergamo carried out several tests [19-25] and is still carrying out quasi-static and fatigue tests in different media in order to evaluate the mechanical and the chemical driving forces involved during fatigue phenomena on Ti-6Al-4V. Furthermore, in [26] Baragetti *et al.* presented a numerical methodology in order to evaluate the crack propagation curves of the tested specimens. A comparison with literature data was also carried out.

An experimental campaign on more than 70 specimens is here described in order to evaluate the involved driving forces. Fatigue and stress corrosion cracking (SCC) tests were carried out and each test took about a week for a total time of about 70 weeks.

The fatigue life of the used specimens was calculated also by means of crack propagation monitoring.

NOMENCLATURE

a crack depth (mm)

N number of cycles

f frequency (Hz)

ΔK stress intensity factor range (MPa$\sqrt{m}$)

ΔK_{th} threshold stress intensity factor range (MPa$\sqrt{m}$)

$\mathbf{\Delta K_{SCC}}$ threshold stress intensity factor range for stress corrosion cracking (MPa$\sqrt{\text{m}}$)
R load ratio during the fatigue tests
ρ root dimension (mm)
UTS ultimate tensile strength (MPa)
YS yield strength (MPa)
E Young modulus (MPa)
A% elongation (per cent)
$\mathbf{K_t}$ stress concentration factor
$\mathbf{\sigma_{max}}$ fatigue limit for the fatigue tests (MPa)
$\mathbf{\sigma_{final}}$ maximum nominal stress during the last step (MPa)
$\mathbf{\sigma_{prior}}$ maximum nominal stress during the step before the last (MPa)
$\mathbf{N_f}$ number of cycle to failure

2. Materials and methods

Figure 2 and Figure 3 show the geometry of the V-notched and the smooth (i.e. with small stress concentration factors) specimens employed for the analysis. The samples were originated by two rolled plates with this average chemical composition (wt.%): 5.97 Al, 4.07 V, 0.20 Fe, 0.19 O, 0.003 C, 0.015 H, 0.05 N and Ti bal. The notch axis was parallel to the rolling direction and the specimens were subjected to a STOA (Solution Treatment and Over-Aging) treatment which consists of a 1 h solution treatment (925°C) and following over-aging carried out by means of a 2 h vacuum annealing (700°C).

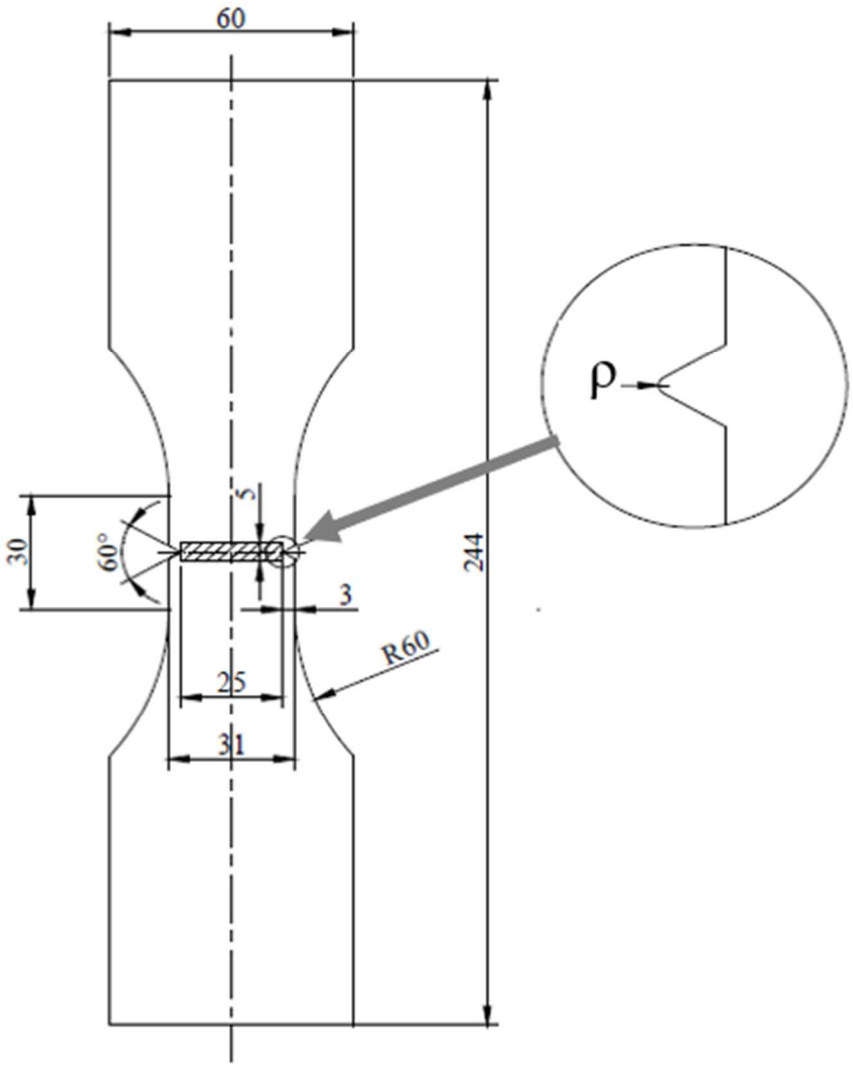

Figure 2 V-notched specimens.

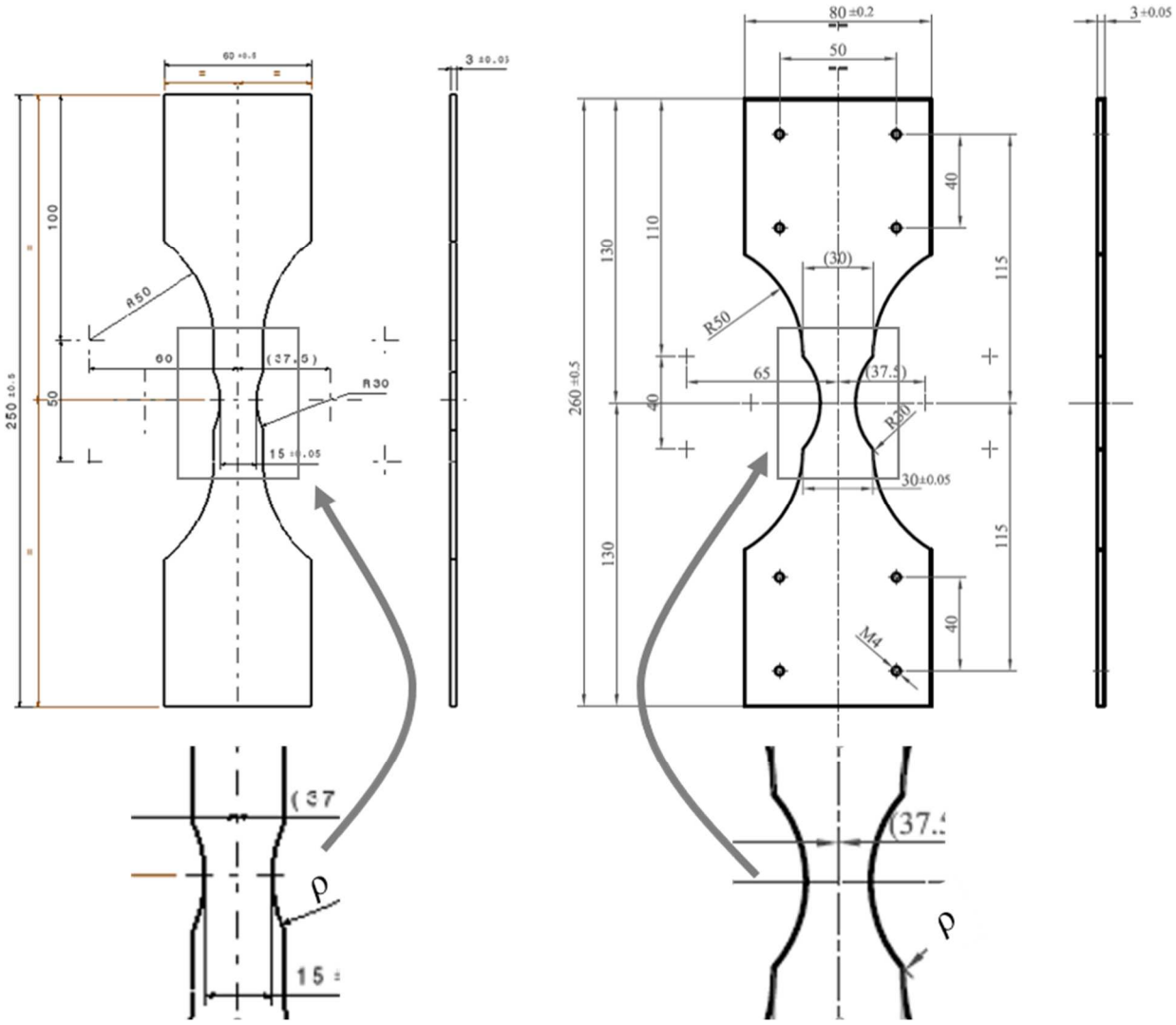

Figure 3 Smooth specimens: K_t=1.18 (left) and K_t=1.16 (right).

The mechanical characteristics of the specimens before and after the STOA treatment are shown in Table 1.

Table 1. Mechanical characteristics before and after the STOA treatment.

	UTS (MPa)	YS (MPa)	E (MPa)	A%
Before STOA	1000-1100	958-1050	110000	16
After STOA	947-990	900-945		

Milling at low cutting speed in order to minimize residual stresses and an electrical discharge machining (EDM) were used for the realization of the roots. A final 1 h stress relaxation (700°C) took away the residual stresses.

The stress concentration factors K_t for the different notches were calculated by 2D linear elastic finite element (FE) modelling with plane-strain elements and are reported in Table 2. The actual notch dimension was measured by means of optical microscope observations.

Table 2 Stress concentration factor for the different roots.

ρ [mm]	30 (smooth)		2.5	1.5	0.45	0.26	0.06	0.05	0.025
K_t	1.16	1.18	2.55	3.10	5.17	6.63	13.34	14.34	18.65

The specimens were tested in different media: laboratory air, paraffin oil, laboratory air + beeswax coating (inert environment), 3.5 wt.% NaCl solution (aggressive environment) and water-methanol solutions with different concentration (aggressive and very aggressive environments).

Two specimens were experienced for each geometry-environment combination in order to confirm the first results.

2.1. Fatigue tests

The tests were conducted on universal testing machines:

- BRT T1000
- INSTRON 1273
- WALTER + BAI LFV250 – T2200 (rented)
- MTS 319.10 (rented).

The specimens were subjected to axial fatigue tests with $R = 0.1$ and $f = 10$ Hz. The aim of these experiments was to evaluate the fatigue limit for a life of $2 \cdot 10^5$ load cycles.

A step loading procedure [9] was applied. The specimens were mounted on the machine and subjected to a prefixed initial load equal to the load for the considered number of cycles on the literature Haigh diagrams decreased of a chosen percentage.

The step loading procedure consists in the repetition of the tests with increasing load (5-20%) until the rupture of the sample occurs. The maximum stress limit at the complete fracture is calculated by a linear interpolation presented in Lanning *et al.* [8-9]:

$$\sigma_{max} = \sigma_{prior} + \frac{N_f}{2 \cdot 10^5} (\sigma_{final} - \sigma_{prior}) \quad (1)$$

where σ_{final} is the maximum nominal stress in the minimum cross section without the presence of the notch during the last step;

σ_{prior} is the maximum nominal stress during the previous step;

N_f is the number of cycles to failure in the last loading step.

If the failure occurs during the first loading step, the maximum stress is the linear interpolation between the stress of the single step and the load decreased by a prefixed quantity such as the specimen was subjected to a zero step with this last load.

2.2. SCC tests

A system made of a threaded link support and a nut which apply the load was used for the quasi-static tests. An increasing load with a rate of about 5 MPa/hour was chosen.

New grips with spherical joints were specially designed in order to avoid unwanted bending moments (Figure 4).

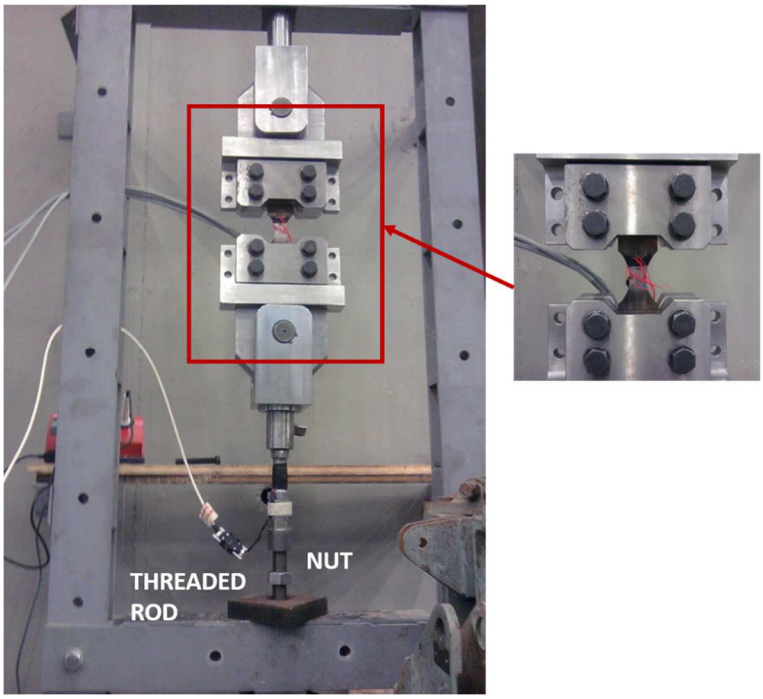

Figure 4 SCC machine, new grips.

2.3. Fatigue tests: device for the complete immersion in the medium

The complete immersion of the central zone of the specimen in the individual corrosive solution was guaranteed for each test by means of a watertight cell and a recirculation system which continuously pumped the medium (Figure 5). The cell was composed by two pieces in order to allow its opening so that the crack nucleation (i.e. initiation) and propagation could be monitored while the specimen was still on the machine during the test.

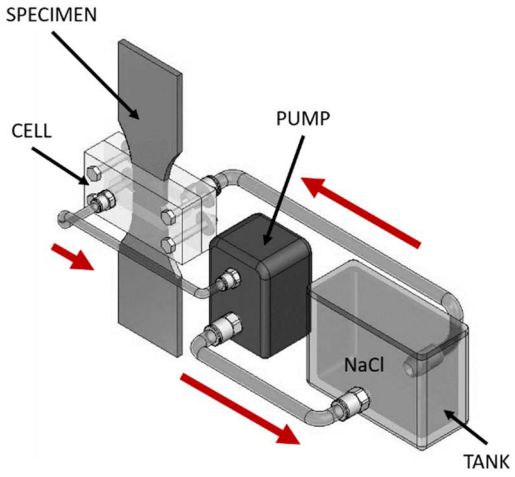

Figure 5 Recirculating device for complete immersion.

2.4. Crack nucleation and propagation

Crack nucleation and propagation were investigated by means of the replica method. Small acetate strips whose thickness was a few tenth of a mm were sited every 5,000, 10,000 or 20,000 cycles in correspondence of the crack zone. The application of the strips was more frequent as soon as the crack nucleated. The surface was previously polished and the strips were softened in acetone for about 5 seconds before the application. This phase took about 20 seconds so that the acetate could penetrate in the crack and reproduce its shape. The strips were removed in order to let the solvent evaporate. The replicas were then observed by means of an optical microscope (LEICA OPTO – 112401 optical microscope).

The crack propagation was also monitored by means of some crack gages. They are parallel resistors oriented perpendicularly to the specimen axis. Because of the crack propagation the rupture of some strands occurs and

the resistance becomes grower as the crack becomes bigger [27]. Figure 6 shows the results of the replica method on a specimen with $K_t = 3.1$.

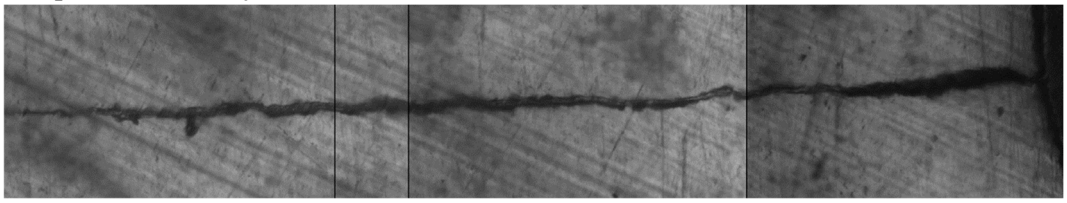

Figure 6 Replica method applied to a specimen with $K_t = 3.1$ tested in laboratory air, estimated crack depth of 3439 μm, 65,069 cycles.

A Scanning Electron Microscope (SEM) analysis of the fracture surfaces was carried out by means of ZEISS-EVO50 in order to highlight the influence of the stress concentration factor and the environment and an optical LEICA OPTO43-112401 (400x) metallographic microscope was adopted in order to observe the replicas and the specimens in the machines.

3. Results

3.1. Fatigue tests

For the fatigue tests in air and in saline solution, SEM analysis showed similar surfaces. The α grains, due to the heat treatment, occupied about 50% of the surface and their dimensions were about 30 μm (Figure 7). They are responsible of the early crack propagation.

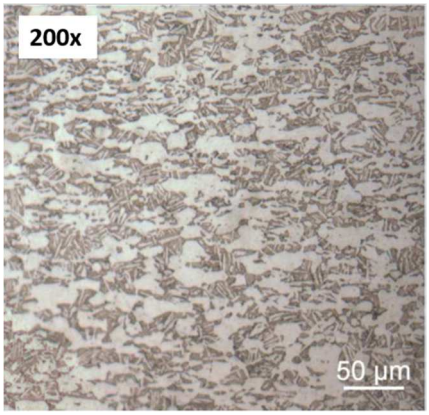

Figure 7 Microstructure of Ti-6Al-4V after the STOA treatment, transversal direction.

The crack propagation rate is higher in NaCl solution, especially for high loads. The surface became smoother for high K_t values (Figure 8). The reason of this behavior can be reached in the meaning of K_t: high stress concentration factors mean small applied load on the specimen for crack nucleation at the notch tip but also small gradients far away. The gradients are the driving force for crack propagation.

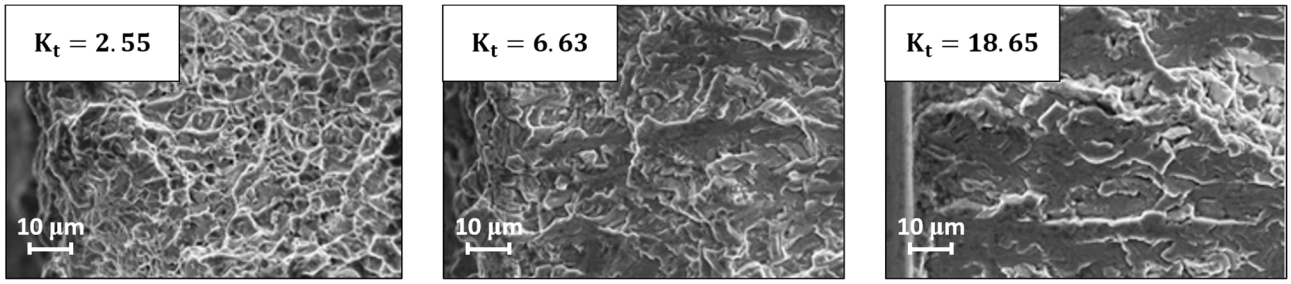

Figure 8 Surface morphology for different stress concentration factors in NaCl, 2500x.

Figure 9 points out that the saline solution reduced the maximum strength of about 20 % (more for low stress concentration factors). The modifications were not probably so appreciable because the fast crack propagation might inhibit corrosion attacks. For the same reason the surfaces are similar.

The beeswax was used in order to analyze other inert environments and gave the same results of paraffin oil and air. Paraffin oil has however such a better performance for high stress concentration factors.

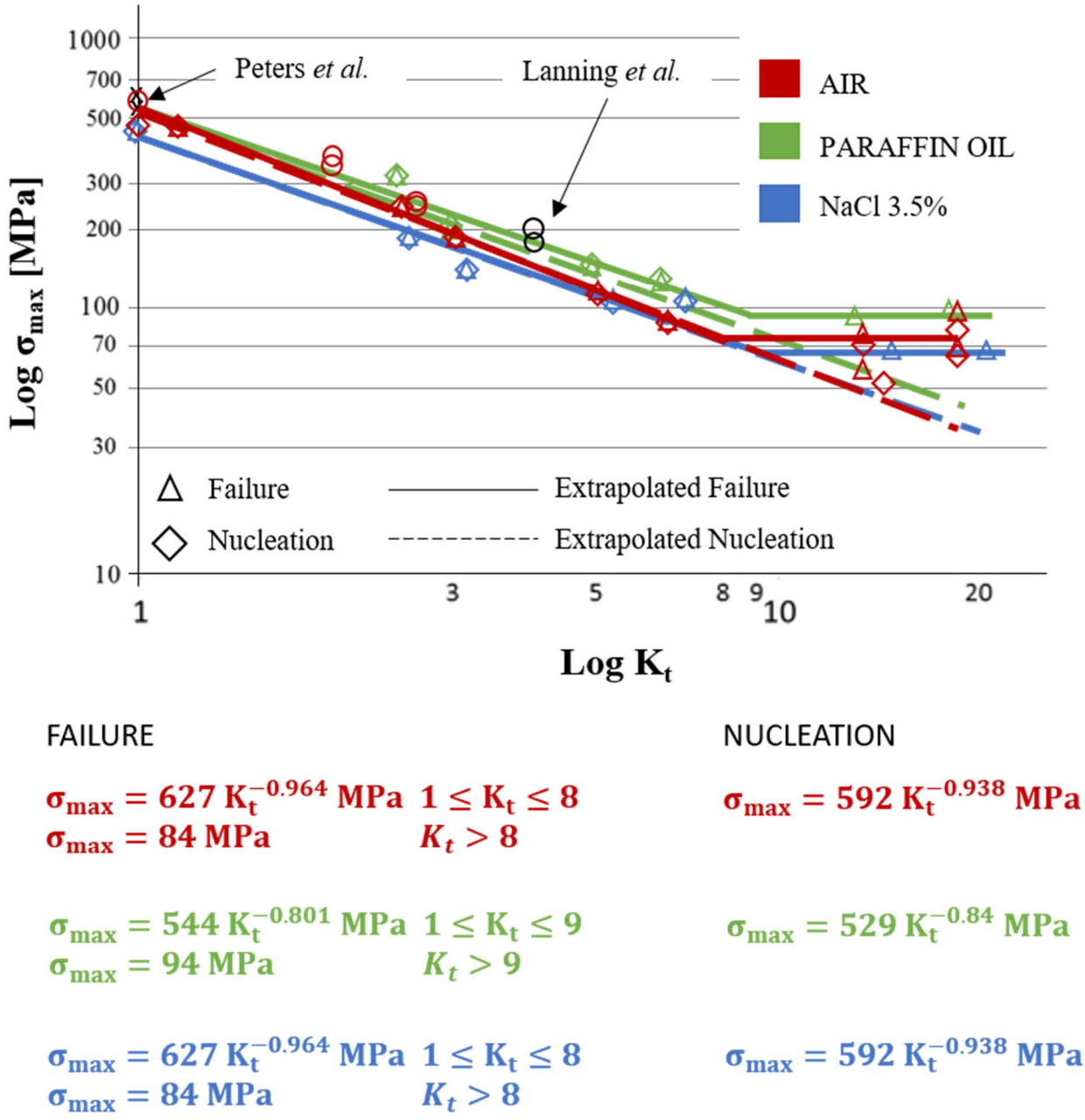

Figure 9 Maximum stress vs $K_t = 1.18$.

Figure 9 shows also that the maximum stress decreases for increasing stress concentration factor until $K_t = 8 - 9$ for all the investigated environments. For stress concentration factors higher than this threshold, the maximum stress to failure is constant. This behavior is in accordance with Frost *et al.* [28] where the effect of the stress concentration factor on fatigue life (number of cycles equal to 200,000 also in this case) for mild steel was analyzed and a threshold equal to 3-4 was found. The reduction is of 80-85% in correspondence of this threshold.

Table 3 summarizes the initial crack depth for all the specimens. The missing value are due to temporary out of order of the microscope or overloads occurred during the tests.

Table 3 Measured initial crack depth [mm].

K_t	air	NaCl	paraffin
2.55	1240	2366	1080
2.55	1240		
3.1	922	7627	1481

3.1	922	16163	915
5.17	562	611	330
5.17	684	5734	
6.63	155	1350	95
6.63	1051	1920	
13.34	548	264	341
13.34		569	652
14.34	32		
14.34			
18.65	186	211	
18.65		242	

It has to be noted that in some cases the rupture occurred in sections far from the minor area. Therefore the maximum stress was calculated using the actual involved area.

The methanol had a very aggressive action, with a mean reduction of 24% for a methanol concentration of 5%, 36% for 25%, 45% for 50% and 56% for 95% (Figure 10). As the methanol concentration grows, the dispersion of the results decreases because the corrosive attacks might be more probable. For the specimens in methanol we have two limits:

- Upper limit: $\sigma_{max} = 0.0261x^2 - 5.0768x + 496.51$ (coefficient of determination $R^2 = 0.999$)
- Lower limit: $\sigma_{max} = 0.011x^2 - 2.2681x + 343.14$ ($R^2 = 0.916$).

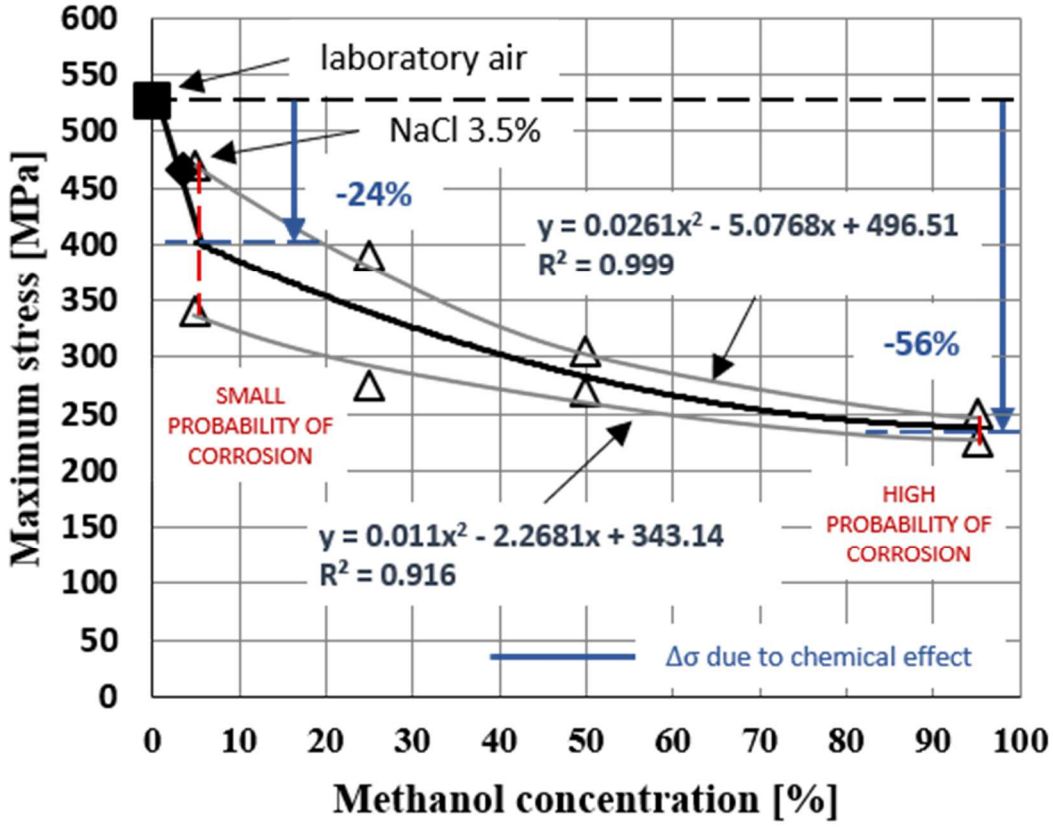

Figure 10 Maximum stress vs methanol concentration ($K_t = 1.18$).

3.2. SCC tests

Fatigue tests pointed out the effects of the coexisting mechanical and chemical forces. For this reason, the quasi-static tests were performed in order to evaluate the exclusive chemical driving force.

The effects of the environment were not so detrimental as in the previous tests. Only methanol concentrations higher than 90% gave sensible reduction of resistance (25%,Figure 11). The maximum stress to failure became

810 MPa for smooth specimen with $K_t = 1.16$ in 95% water-methanol solution against 895 MPa for the same specimen in air (Table 3), while about 670 MPa for $K_t = 1.18$ and 99.8% methanol concentration against 900 MPa for the same sample in air. The trend can be considered linear and is between

- $y = 945\ MPa$ for Methanol concentration<90%
  $y = -22.5x + 2965\ MPa$ for Methanol concentration>90%
- $y = 875\ MPa$ for Methanol concentration<85%
  $y = -18.5x + 2480$ for Methanol concentration>85%

Transgranular cracks can be seen in the α-enriched layer on the outer surface and the corrosion attacks for high methanol concentrations gave smoothed surfaces (Figure 12).

Table 3 Maximum stress, $K_t = 1.16$.

	σ_{max} [MPa]
Air	895
NaCl 3.5%	885
Methanol 95%	810

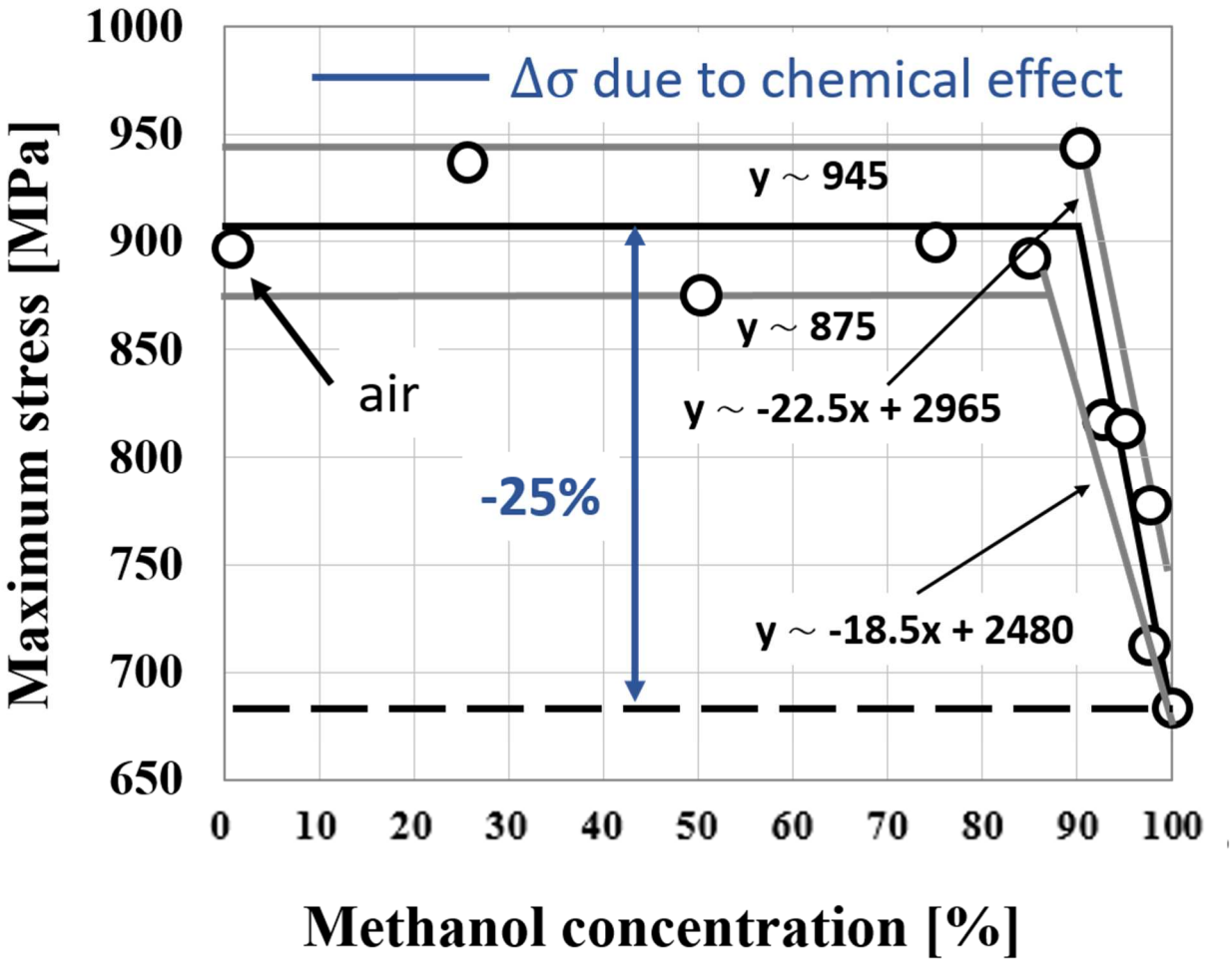

Figure 11 Maximum stress vs methanol concentration ($K_t = 1.18$).

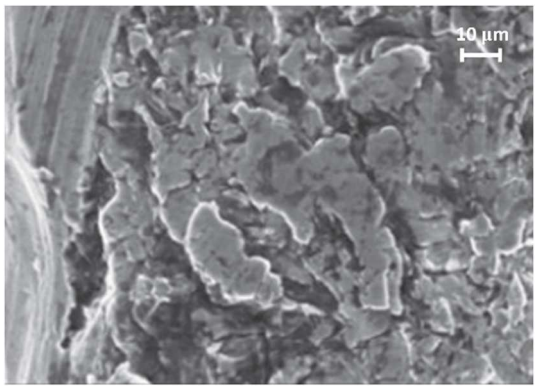

Figure 12 Surface morphology for 95% methanol, $K_t = 1.18$.

4. Conclusions

V-notched and smooth ($K_t = 1.16$ and $K_t = 1.18$) specimens were employed in order to analyze SCC and corrosion fatigue behavior of Ti-6Al-4V and evaluate the environmental and mechanical forces involved during fatigue phenomena in inert (air and paraffin oil), aggressive and very aggressive (saline and methanol solutions with different concentrations) environments. The axial fatigue tests were carried out at a frequency equal to 10 Hz and a load ratio equal to 0.1. The objective of the tests was to determine the maximum stress to failure for 200,000 load cycles by means of the step-loading procedure.

Finite elements models were built in order to calculate K_t and crack propagation rate was monitored by means of the replica method.

The SEM inspection showed the effects of the different media and of the stress concentration factor on the surface morphology.

In particular it can be stated that:

- Air and paraffin oil have the same effects;
- 3.5%wt. NaCl solution gives a reduction of about 20% for all the stress concentration factors in fatigue tests;
- The morphology of the surface for the specimens in air and the saline solution are similar probably because of the fast propagation of the crack which inhibits the corrosion;
- For all the tested environments a threshold value of K_t was discovered. For value above 8-9 the maximum stress to failure is constant;
- As the K_t increases the surface becomes smoother accordingly to the definition of stress concentration factor and the consequent value of stress at the notch tip and the gradient of stresses;
- High methanol concentrations give detrimental reduction of the fatigue limit (-56% for 95%wt. methanol solution) but also small concentration have conspicuous effects (-24% for 5%wt.) so no passivation action occurs even for small quantities of methanol;
- The significant values reported in the previous point are due to the mechanical and chemical forces. If we consider only the chemical force, we have a decrement of the maximum stress only for concentration higher than 90% with a reduction of 25% for 99.8%wt. concentration.

Thus it can be generally concluded that variable loads combined to aggressive environments decrease the strength of the Ti-6Al-4V alloy more than the aggressive environments.

The future activities of the SMLab could involve the study of the effects of overload on the crack initiation period as presented in Milikota *et al.*[29]. Another interesting issue could be the study of the combined action of the environment and the frequency.

5. References

[1] Brown B.F. Stress Corrosion Cracking in High-Strength Steels and in Titanium and Aluminum Alloys, 1972: 147–244, Naval Research Laboratory, Washington, D.C.

[2] Lee E.U., Vasudevan A.K., Sadananda K. Effects of various environments on fatigue crack growth in Laser formed and IM Ti-6AI-4V alloys. International Journal of Fatigue 2005; 27: 1597-1607.
[3] Johnston R.L., Johnson R.E., Ecord G.M., Castner W.L. Stress-Corrosion Cracking of Ti-6al-4V Alloy in Methanol, NASA Technical Note TN D-3868, 1967.
[4] Johnson, R.E. NASA Experiences with TI-6Al-4V In Methanol, DMIC Memorandum 228, 1967.
[5] Morrissey R.J., McDowell D.L, Nicholas T. Frequency and stress ratio effects in high cycle fatigue of Ti-6Al-4V. International Journal of Fatigue 1999; 21, 7: 679-685.
[6] Ritchie R.O., Boyce B.L., Campbell J.P., Roder O., Thompson A.W., Milligan W.W., Thresholds for high-cycle fatigue in a turbine engine Ti–6Al–4V alloy. International Journal of Fatigue 1999; 21: 653-662,.
[7] Morrissey R.J, Nicholas T. Fatigue strength of Ti–6Al–4V at very long lives. International Journal of Fatigue 2005; 27, 10-12: 1608-1612.
[8] Lanning D.B., Nicholas T., Palazotto A. The effect of notch geometry on critical distance high cycle fatigue predictions. International Journal of Fatigue 2005; 27, 10-12: 1623-1627.
[9] Lanning D.B., Nicholas T., Haritos G.K. On the use of critical distance theories for the prediction of the high cycle fatigue limit stress in notched Ti–6Al–4V. International Journal of Fatigue 2005; 27: 45-57.
[10] Gubeljak N., Cvetic, M., Bozic Z, Predan J. Application of structural integrity assessment procedure on an axle pin of a wind turbine," Fatigue & Fracture of Engineering Materials & Structures 2017; 40, 8: 1284-1294.
[11] Bellows R.S., Muju S., Nicholas T. Validation of the step test method for generating Haigh diagrams for Ti-6Al-4V. International Journal of Fatigue 1999; 21, 1: 687-697.
[12] Haritos G.K., Nicholas T., Lanning D. B. Notch size effects in HCF behavior of Ti-6Al-4V. International Journal of Fatigue 1999; 21, 7: 643-652.
[13] Peters J.O., Boyce B.L., Chen X., McNaney J.M., Hutchinson J.W., Ritchie, R.O. On the application of the Kitagawa–Takahashi diagram to foreign-object damage and high-cycle fatigue, Engineering Fracture Mechanics 2002; 69, 13: 1425–1446.
[14] Leuders S., Thöne M., Riemer A., Niendorf T., Tröster T., Richard H., Maierad H. On the mechanical behaviour of titanium alloy TiAl6V4 manufactured by selective laser melting: Fatigue resistance and crack growth performance. International Journal of Fatigue 2013; 48: 300-307.
[15] Kahlin M., Ansell H., Moverarem J. Fatigue behaviour of additive manufactured Ti-6Al-4V, with as-built surfaces, exposed to variable amplitude loading. International Journal of Fatigue 2017; 103: 353-362.
[16] Seifi M., Salem A., Satko D., Shaffer J., Lewandowski J.J. Defect distribution and microstructure heterogeneity effects on fracture resistance and fatigue behavior of EBM Ti–6Al–4V. International Journal of Fatigue 2017; 94:263-287.
[17] Dawson D., Pelloux R.M. Corrosion fatigue crack growth of titanium alloys in aqueous environments. Metallurgical Transactions 1974; 5, 3: 723-731.
[18] Htoo A.T., Miyashita Y., Otsuka Y., Mutoh Y., Sakurai S. Notch fatigue behavior of Ti-6Al-4V alloy in transition region between low and high cycle fatigue. International Journal of Fatigue 2017; 95: 194-203, 2017.
[19] Baragetti S., Foglia C., Gerosa R. Fatigue Crack Nucleation and Growth Mechanisms for Ti-6Al-4V in Different Environments. Key Engineering Materials 2013; 525-526: 505-508.
[20] Baragetti S., Villa F. Quasi-Static Behavior of Notched Ti-6Al-4V Specimens in Water-Methanol Solution. Corrosion Reviews 2015; 33, 6: 477-485.
[21] Baragetti S., Villa F. SCC and corrosion fatigue characterization of a Ti-6Al-4V alloy in a corrosive environment – experiments and numerical models. Frattura ed Integrità Strutturale 2014; 8, 30: 84–94.
[22] Baragetti S., Villa F. Corrosion Fatigue of High-Strength Titanium Alloys Under Different Stress Gradients. The Journal of The Minerals, Metals & Materials Society (JOM) 2015; 67, 5: 1154-1161.
[23] Baragetti S., Medolago, A. Load and environmental effects on the corrosion behavior of a Ti-6Al-4V, Key Engineering Materials 2013; 525-526: 501-504.
[24] Baragetti S. Notch Corrosion Fatigue Behavior of Ti-6Al-4V. Materials 2014; 7 (6): 4349-4366.

[25] Arcieri E.V., Baragetti S. SCC and corrosion fatigue sensitivity of Ti-6Al-4V alloy. ICSID 2017 Conference. Dubrovnik, Croatia.
[26] Baragetti S., Villa F. Crack propagation models: numerical and experimental results on Ti–6Al–4V notched specimens. Fatigue & Fracture of Engineering Materials & Structures 2016; 40, 8: 1276-1283.
[27] HBM. Strain gages and Accessories. 2015.
[28] Frost N. E., Dugdale D. S. Fatigue tests on notched mild steel plates with measurements of fatigue cracks. Journal of the Mechanics and Physics of Solids 1957; 5, 3: 182-192.
[29] Milikota M., Schmauder S., Bozic, Z., Hummel, M. Modelling of overload effects on fatigue crack initiation in case of carbon steel. Fatigue & Fracture of Engineering Materials & Structures 2017; 40, 8: 1182-1190.